AD_____
(Leave blank)

Award Number: W81XWH-08-1-0113

TITLE: Imaging Heat Shock Protein 90 (Hsp90) Activity in Hormone-Refractory Prostate Cancer

PRINCIPAL INVESTIGATOR: Niu, Gang Ph.D.

CONTRACTING ORGANIZATION: Leland Stanford Junior University
Stanford, CA 94305-4125

REPORT DATE: March 2009

TYPE OF REPORT: Annual Summary

PREPARED FOR: U.S. Army Medical Research and Materiel Command
Fort Detrick, Maryland 21702-5012

DISTRIBUTION STATEMENT: (Check one)

X Approved for public release; distribution unlimited

☐ Distribution limited to U.S. Government agencies only; report contains proprietary information

The views, opinions and/or findings contained in this report are those of the author(s) and should not be construed as an official Department of the Army position, policy or decision unless so designated by other documentation.

REPORT DOCUMENTATION PAGE

Form Approved
OMB No. 0704-0188

1. REPORT DATE *(DD-MM-YYYY)*	**2. REPORT TYPE**	**3. DATES COVERED** *(From - To)*
24/03/2009	Annual Summary	02/25/2008 to 02/24/2009

4. TITLE AND SUBTITLE
Imaging Heat Shock Protein 90 (Hsp90) Activity in Hormone-Refractory Prostate Cancer

5a. CONTRACT NUMBER
W81XWH-08-1-0113

5b. GRANT NUMBER
PC073549

5c. PROGRAM ELEMENT NUMBER

6. AUTHOR(S)
Niu, Gang

Chen, Xiaoyuan

5d. PROJECT NUMBER

5e. TASK NUMBER

5f. WORK UNIT NUMBER

7. PERFORMING ORGANIZATION NAME(S) AND ADDRESS(ES)
Leland Stanford Junior University
Stanford, CA 94305-4125

8. PERFORMING ORGANIZATION REPORT NUMBER

9. SPONSORING / MONITORING AGENCY NAME(S) AND ADDRESS(ES)
U.S. Army Medical Research and Materiel Command
Fort Detrick, Maryland 21702-5012

10. SPONSOR/MONITOR'S ACRONYM(S)

11. SPONSOR/MONITOR'S REPORT NUMBER(S)

12. DISTRIBUTION / AVAILABILITY STATEMENT
Approved for public release; distribution unlimited

13. SUPPLEMENTARY NOTES

14. ABSTRACT

During the first year of the funding period, we have labeled 1, 3-propoyldiamine modified geldanamycin with both fluorescent core (FITC in this case) and radioisotopes. Unfortunately, in vitro cell experiments failed to disclose the ability of FITC-GM to monitor Hsp90 activity changes after heat stimulation in prostate cancer cell lines. Small molecular Hsp90 inhibitors, at least GM derivatives, showed reasonable tumor accumulation after being labeled with ^{64}Cu. However, in vitro experiments revealed that the GM derivatives are insufficient to tell the changes of both Hsp90 level and activity after stimulation. It might be more appropriate to use GM imaging for tumor detection instead of Hsp90 activity monitoring.

Therefore, we switched gears to monitor Hsp90 activity indirectly through imaging downstream client proteins including EGFR and HER2 expression by ^{64}Cu labeled antibodies. Hsp90 activity can be evaluated indirectly by imaging one or several of its downstream client proteins. The quantitative PET imaging of EGFR expression with ^{64}Cu-DOTA-cetuximab is successful for monitoring the early therapeutic response upon 17-AAG treatment in a human prostate cancer PC-3 tumor model. The quantification of EGFR degradation upon 17-AAG treatment using PET imaging is consistent with other in vitro and ex vivo measurements. This strategy may be applied to monitor the therapeutic response in EGFR-positive cancer patients under 17-AAG treatment.

15. SUBJECT TERMS

16. SECURITY CLASSIFICATION OF:			**17. LIMITATION OF ABSTRACT**	**18. NUMBER OF PAGES**	**19a. NAME OF RESPONSIBLE PERSON**
a. REPORT	**b. ABSTRACT**	**c. THIS PAGE**			USAMRMC
U	U	U	UU	14	**19b. TELEPHONE NUMBER** *(include area code)*

Table of Contents

Page

INTRODUCTION

Based on the extremely important function of Hsp90 in the survival and proliferation of tumor cells, the therapy focusing on Hsp90 inhibition will become a potentially important prostate cancer treatment strategy, especially for refractory prostate cancers. In the research proposal, we hypothesized that Hsp90 activity, *i.e.* the amount of active form of Hsp90, is the main determining factor for the response to Hsp90 inhibition therapy. The first goal is to develop probes to monitor Hsp90 activity non-invasively. We speculated that PET imaging with suitably radiolabled Hsp90 substrates will be highly valuable in assessing Hsp90 activity non-invasively and repetitively. The major objective of this 2-year training proposal is to image prostate cancer Hsp90 activity in vivo.

During the first year of the funding period, we have labeled 1, 3-propoyldiamine modified geldanamycin with both fluorescent core (FITC in this case) and radioisotopes. Unfortunately, in vitro cell experiments failed to disclose the ability of FITC-GM to monitor Hsp90 activity changes after heat stimulation in prostate cancer cell lines. The emerging literature also revealed that highly nonspecific cellular binding is the main barrier for the hyperlipophilic small molecules including GM. Therefore, we switched gears to monitor Hsp90 activity indirectly through imaging downstream client proteins including EGFR and HER2 expression by ^{64}Cu labeled antibodies. Reporter gene based Hsp90 activity measurement is in progress to further clarify the mechanism of anti-Hsp90 therapy and for potential drugs screening.

BODY

Part I. GM derivatives failed to detect Hsp90 activity changes

Geldanamycin (GM) was reacted with 1,3-propoyldiamine to afford 17-trimethylenediamine-17-demthyoxygeldanamycin (TD), which was then conjugated with activated DOTA ester to afford DOTA-TD) for ^{64}Cu labeling. Mice bearing human glioma U87MG tumors were then subjected to microPET scans at various time points post-injection (p.i.) of ^{64}Cu-DOTA-TD. The coronal slices that contain the tumor are shown in **Fig. 1.** The uptake of ^{64}Cu-DOTA-TD into U87MG tumor was rapid and high, reaching a peak at 18 h p.i. Liver and kidney also exhibited relatively high tracer uptake. The uptake in most other organs was at very low level. The uptake in the kidneys dropped steadily over time **(Fig. 1).**

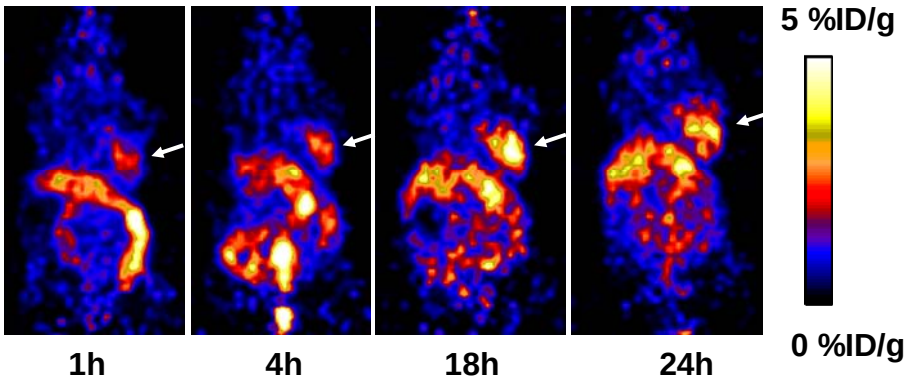

Fig. 1. MicroPET imaging of Hsp90 activity by ^{64}Cu-DOTA-TD in U87MG tumor-bearing nude mice (arrow).

After this initial success of labeling Hsp90 substrate for PET imaging, we performed in vitro experiments to explore whether the uptake of ^{64}Cu-DOTA-TD is related to Hsp90 protein level and Hsp90 ATPase activity. For in vitro uptake assay, 1 x 10^5 PC-3 cells were seeded in 24-well plates 48 h prior to uptake assay. In the stress group, cells were cultured in serum free medium (SFM) for 24 h. Then 18.5 kBq of ^{64}Cu-labeled GM was added to each well in 0.5 ml of SFM. At different time points after adding ^{64}Cu-GM, the medium was removed and the cells were washed twice with 1 ml of ice-cold PBS. Finally cells from each well were collected and the radioactivity (counts per minute) was measured with a gamma counter (Cobra II, Packard, USA). The results were shown in **Fig. 2.** The accumulation of ^{64}Cu-DOTA-GM increased along with time. Compared with control cells, however, the stressed PC-3 did not show significantly higher uptake of ^{64}Cu-DOTA-GM.

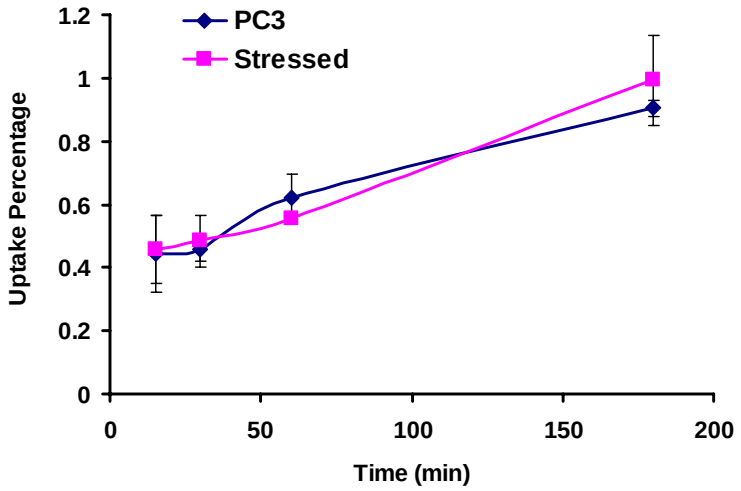

Fig. 2. Uptake assay of ^{64}Cu-GM in PC3 cells

We further modified GM and labeled it with FITC according to the reaction scheme provided in **Fig. 3A**. We then stimulated Hsp90 expression and activation in both PC3 and 22RV1 cells by heat or phorbol 12-myristate-13-acetate (PMA). Still, we did not observe significant difference of signal intensity visualized by fluorescence microscope **(Fig. 3B)**.

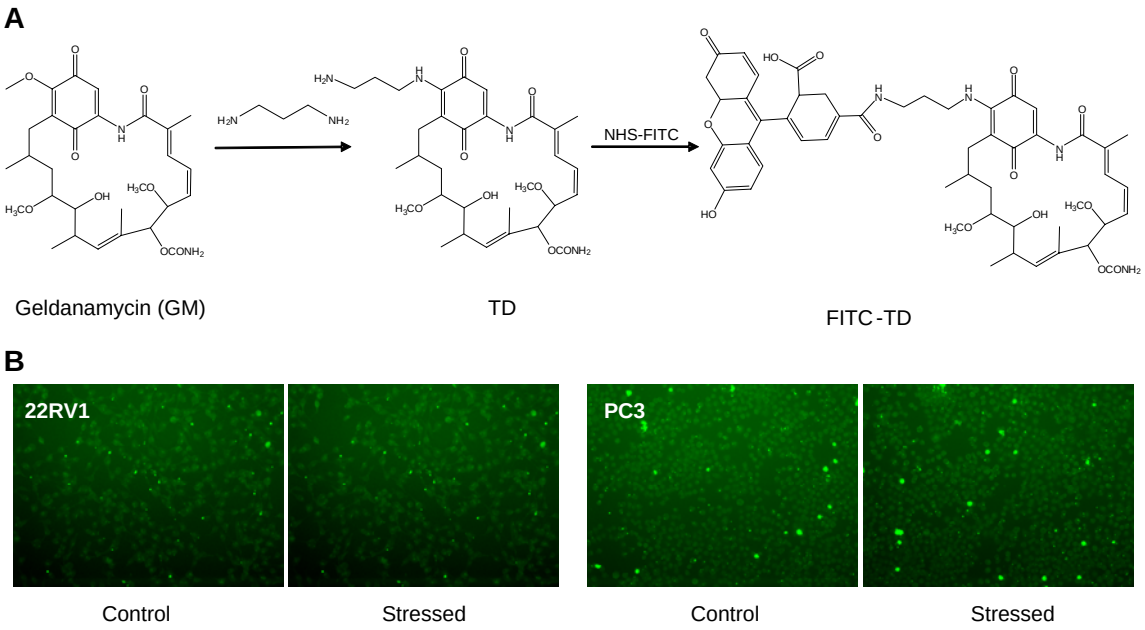

Fig. 3. (A) Synthesis of FITC-GM; **(B)** Monitoring Hsp90 activity with FITC-GM in prostate cancer cell lines.

We concluded from above experiments that it might be difficult to image Hsp90 activity with GM derivatives due to its hyperlipophicity as reported by Su *et al.* (Eur J Nucl Med Mol Imaging. 2008; 35:1089-99). Consequently, we pursued indirect imaging of Hsp90 activity with ^{64}Cu-labeled EGFR antibody instead of GM derivatives.

PART II. Non-invasive PET imaging of EGFR degradation induced by a heat shock protein 90 inhibitor

After being treated with Hsp90 inhibitor, the downstream client proteins such as EGFR, HER2 would be downregulated. However, HER-2 expression is typically low in tumors except for breast and ovarian tumors, in which HER-2 imaging has only limited applications. PC-3 cells had low HER-2 expression and 17-AAG treatment induced only minimal HER-2 degradation. Thus, we chose to image EGFR degradation with ^{64}Cu labeled cetuximab (Erbitux; C255; ImClone and Bristol-Myers Squibb), a mouse–human chimeric IgG_1 mAb that binds with high affinity to EGFR.

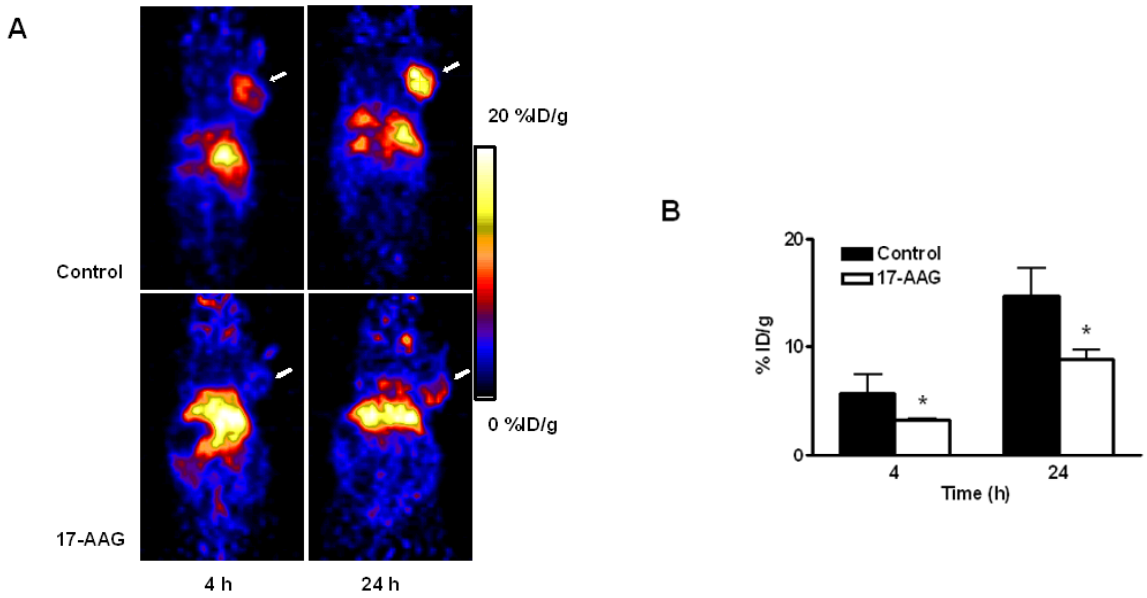

Fig. 4. (**A)** MicroPET images of PC-3 tumor-bearing nude mice at 4 h and 24 h after intravenous injection of ^{64}Cu-DOTA-cetuximab with or without 17-AAG treatment (n = 4/group). Decay-corrected whole-body coronal images that contain the tumor were shown and the tumors are indicated by white arrows. **(B)** PC-3 tumor uptake of ^{64}Cu-DOTA-cetuximab as quantified from microPET scans (n = 4/group). *, $P < 0.05$.

^{64}Cu-DOTA-cetuximab was determined to have 21.5 ± 2.2 DOTA residues per cetuximab and control human IgG_1 had 24.08 ±0.42 DOTA residues (n = 4). The specific activity of ^{64}Cu-DOTA-cetuximab was 1.24 ± 0.13 GBq/mg mAb and the radiolabeling yield was 84.0 ± 8.7% (n = 5). There was minimal reduction in the immunoreactivity of cetuximab after DOTA conjugation. After being treated with 17-AAG for 24 h, the PC-3 tumor uptake of ^{64}Cu-DOTA-cetuximab was much lower in both early and late time points as compared with the untreated group **(Fig. 4A)**. In untreated mice, the PC-3 tumor uptake of ^{64}Cu-DOTA-cetuximab was 5.8 ± 1.7 %ID/g and 14.6 ± 2.6 %ID/g at 4 and 24 h p.i., respectively. The uptake in 17-AAG treated tumors was significantly lower, 3.3 ± 0.3 %ID/g and 8.9 ± 1.6 %ID/g at 4 and 24 h p.i. respectively ($P < 0.05$ at both time points; n = 4) **(Fig. 4B)**. There were no significant differences of ^{64}Cu-DOTA-cetuximab uptake in other major organs between the 17-AAG treated group and untreated animals.

After microPET imaging at 24 h p.i., the animals were sacrificed for biodistribution studies and the results were shown in Fig. 5. The untreated PC-3 tumor had a high tracer uptake of 17.6 ± 5.3 %ID/g, consistent with the non-invasive microPET imaging results. After 17-AAG treatment, the uptake decreased significantly ($P < 0.05$) to 10.1 ± 0.7 %ID/g. The liver also had prominent radioactivity accumulation, with an uptake of 17.1 ± 4.2 %ID/g at 24 h p.i., due to both the hepatic clearance of antibody-based tracer and possible trans-chelation. Blood activity concentration was 7.9 ± 3.1 %ID/g at 24 h p.i., indicating the long circulation life time of the antibody. Compared with ^{64}Cu-DOTA-cetuximab, ^{64}Cu-DOTA-IgG$_1$ has a higher blood concentration (14.3 ± 2.4 %ID/g) and lower liver uptake (7.4 ± 1.8 %ID/g). The non-specific accumulation of ^{64}Cu-DOTA-IgG$_1$ in the PC-3 tumor (due to the leaky vasculature and lack of lymphatic drainage in the tumor) was very low (4.3 ± 0.5 %ID/g at 24 h p.i.; $P < 0.01$ compared with the control), confirming the EGFR specificity of ^{64}Cu-DOTA-cetuximab uptake in the PC-3 tumor.

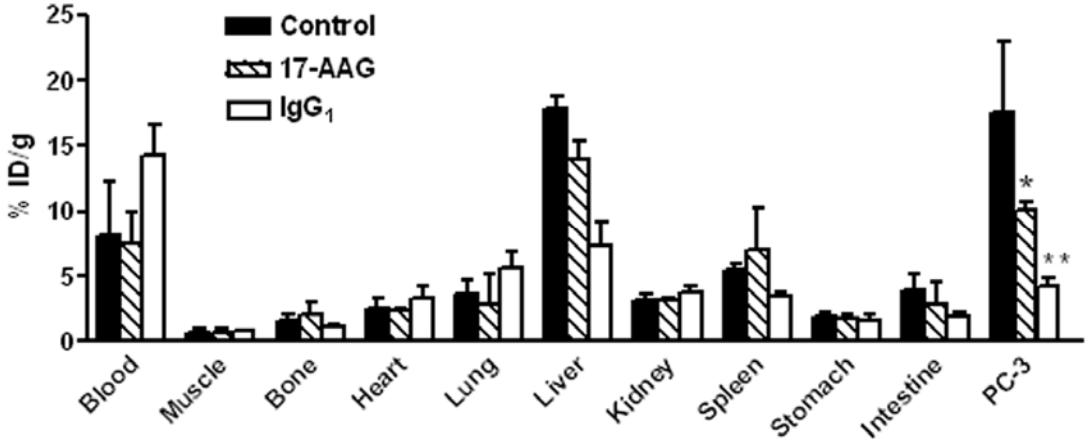

Fig. 5. Biodistribution of ^{64}Cu-DOTA-cetuximab (with or without 17-AAG treatment) and ^{64}Cu-DOTA-IgG$_1$ in PC-3 tumor-bearing mice at 24 h post-injection (n = 4 for each group). *, $P < 0.05$; **, $P < 0.01$.

To further confirm that 17-AAG induces EGFR degradation in vivo, we performed immunofluorescence staining using cetuximab as the primary antibody and Cy3-conjugated donkey anti-human IgG as the secondary antibody. Images were taken under the same condition and displayed at the same scale to make sure that the relative brightness observed in the images reflected the difference in EGFR expression level. In the untreated PC-3 tumor, EGFR expression was very high as indicated by the strong pseudo-colored red signal in the tissue (Fig. 6A). After treated with 17-AAG, EGFR expression was apparently lower with a much weaker fluorescence signal. Western blot of the tumor tissue lysate using cetuximab as the primary antibody also revealed that EGFR expression level in the PC-3 tumor decreased dramatically upon 17-AAG treatment (Fig. 6B). Taken together, biodistribution studies, immunofluorescence staining, and Western blot all confirmed that the decrease in tumor EGFR expression level upon 17-AAG treatment can be non-invasively monitored by ^{64}Cu-DOTA-cetuximab PET.

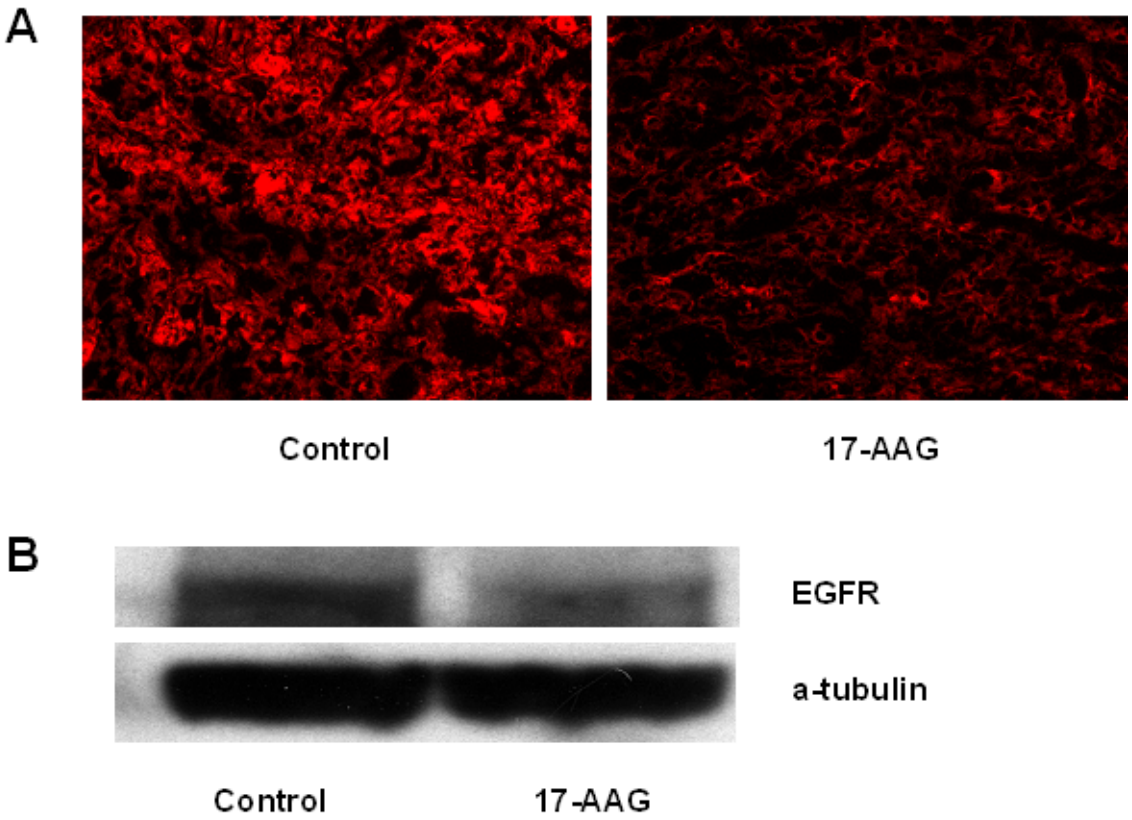

Fig. 6 (A) Immunofluorescence staining of EGFR in 17-AAG treated and untreated PC-3 tumor tissues. Images were obtained under the same conditions and displayed at the same magnification and scale (200×) **(B)** Western blot of EGFR in PC-3 tumors treated or untreated with 17-AAG. Cetuximab was used as the primary mAb.

KEY RESEARCH ACCOMPLISHMENTS

- Developed small molecular Hsp90 inhibitor, GM derivatives, to be used as imaging probes to monitor Hsp90 activity.

- Tested the feasibility of ^{64}Cu-labeled EGFR antibody to image EGFR expression with PET imaging

- Determined that ^{64}Cu-DOTA-cetuximab PET can be used to monitor the early response of EGFR degradation upon anti-Hsp90 therapy by 17-AAG.

REPOERABLE OUTCOMES

1. **Niu G**, Li ZB, Cao Q, Chen X. Monitor Therapeutic Response of Human Ovarian Cancer to 17-DMAG by Non-invasive PET imaging with ^{64}Cu-Trastuzumab. *Eur J Nucl Med Mol Imaging*, Submitted.

2. **Niu G**, Chen X. PET Imaging of Angiogenesis. *PET Clinics*, in press.

3. **Niu G**, Li ZB, Xie J, Le T, Chen X. Imaging Antibody Delivery with microPET in EGFR Positive Head-neck Squamous Cell Carcinoma Models. *J Nucl Med*, in press.

4. **Niu G**, Chen X. Has Molecular and Cellular Imaging Enhanced Drug Discovery. *Drugs R&D*. 2008 9(6):351-368.

5. Cao Q, Cai W, **Niu G**, He L, Chen X. Multimodality Imaging of IL-18bp-Fc Therapy of Experimental Lung Metastasis. *Clin Cancer Res*, 2008 14(19):6137-6145.

6. **Niu G** and Chen X. From Protein-Protein Interaction to Therapy Response: Molecular Imaging of Heat Shock Proteins. *Eur J Radiol*, In press.

7. **Niu G**, Cai W, Chen K, Chen X. Non-Invasive PET Imaging of EGFR Degradation Induced by a Heat Shock Protein 90 Inhibitor. *Mol Imaging Biol*, 2008 10(2):99-106.

8. **Niu G**, Chen X. Noninvasive Visualization of MicroRNA by Bioluminescence Imaging. *Mol Imaging Biol*. 2009;11:61-3.

CONCLUSIONS

Small molecular Hsp90 inhibitors, at least GM derivatives, showed reasonable tumor accumulation after being labeled with ^{64}Cu. However, in vitro experiments revealed that the GM derivatives are insufficient to tell the changes of both Hsp90 level and activity after stimulation. It might be more appropriate to use GM imaging for tumor detection instead of Hsp90 activity monitoring.

Hsp90 activity can be evaluated indirectly by imaging one or several of its downstream client proteins. The quantitative PET imaging of EGFR expression with ^{64}Cu-DOTA-cetuximab is successful for monitoring the early therapeutic response upon 17-AAG treatment in a human prostate cancer PC-3 tumor model. The quantification of EGFR degradation upon 17-AAG treatment using PET imaging is consistent with other in vitro and ex vivo measurements. This strategy may be applied to monitor the therapeutic response in EGFR-positive cancer patients under 17-AAG treatment.

REFERENCES

None

APPENDICES

None